

# Depth/Conversion Characterization of Electron-beam Initiated Polymerization

*Sage Schissel, University of Iowa, Chemical & Biochemical Engineering, Iowa City, USA*

*Stephen C. Lapin, PCT Engineered Systems, LLC, Davenport, USA*

*Julie L. P. Jessop, University of Iowa, Chemical & Biochemical Engineering, Iowa City, USA*

## Abstract

Confocal Raman microscopy was used to determine polymer conversion as a function of depth into electron-beam cured coating samples. Samples were irradiated in atmospheres with varying levels of oxygen. As expected, conversion near the surface increased as the level of oxygen was decreased. Samples were also irradiated under well-inerted conditions while varying the accelerating potential (voltage) of the electron beam. The results show low conversion near the sample bottom at the lower voltages. This lower conversion is consistent with inadequate energy penetration predicted by Monte Carlo simulations.

## Introduction

Electron-beam (EB) curing offers a fast, low-energy, and solvent-free means of polymerizing inks, films, coatings, and adhesives compared to thermal polymerization.<sup>1-3</sup> No initiator is required to form the free-radical active centers, making this technique especially appealing for packaging applications where molecular migration would be problematic. In addition, unlike photopolymerization, additives such as pigments, fillers, fibers, and nanomaterials do not prevent penetration of the ionizing radiation, resulting in excellent product consistency.

EB accelerators used in industrial curing applications operate in the range of 100 to 300 kV. Given a typical carbon-carbon bond energy of 5 eV, there is little selectivity. The ionizing radiation produces a complex mix of reactive radical and ionic sites within the material. These sites can result in polymerization, as well as cross-linking and chain scission.<sup>4</sup> There are a number of commercial applications involving EB-induced polymerization; however, we do not have a fundamental understanding of the polymerization process or how it affects the properties of the polymers that are formed. An increased understanding of EB-induced polymerization would provide guidance for designing performance properties needed for targeted applications.

Published literature in the field of electron-beam (EB) radiation is focused on effects of EB irradiation on polymer and polymer blend properties (i.e., studies with polymers, not during polymerization). There are very few published works on the kinetics of EB polymerizations.<sup>1,2,5,6</sup> Several issues make characterization of EB kinetics particularly challenging. First, the design of the EB system does not lend itself to on-line, real-time monitoring as has been accomplished with photopolymerization systems. Secondly, the EB bombardment is a harsh environment for sensitive monitoring equipment. Third, the web speed of these systems is faster than the time resolution of monitoring equipment suitable for an industrial environment. Raman confocal microscopy may provide quantitative information on chemical changes and conversion that will enable development of initiation and propagation models and determination of structure-property relationships. In this proof-of-concept

study, results demonstrate how nitrogen inerting and voltage change the conversion profile of an EB-cured polymer sample as a function of depth.

## Experimental

### Materials

The formulation was a 50/50 mixture (by weight) of trimethylolpropane triacrylate monomer (TMPTA, Cytec) and bisphenol-A-diglycidylether diacrylate oligomer (BADGEDA, Cytec Ebecryl 3700) (Figure 1). In UV systems, 0.5 wt% of the photoinitiator 2,2-dimethoxy-2-phenylacetophenone (DMPA, Aldrich) was added. All chemicals were used as received.

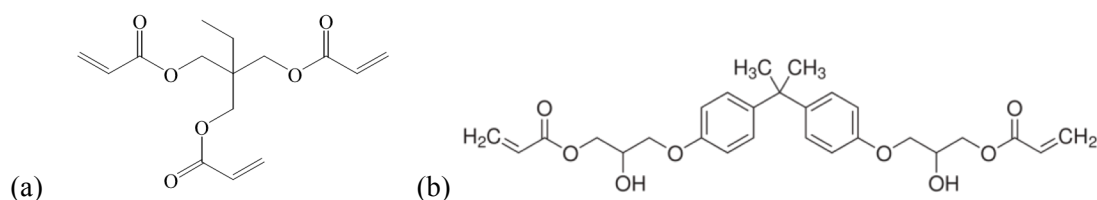


**Figure 1.** Chemical structure of (a) TMPTA and (b) BADGEDA.

### Methods

#### *EB Curing*

The coatings were made on aluminum Q-panels using a 52-rod drawbar and EB-cured using a BroadBeam EP Series electron-beam accelerator equipped with a variable speed fiber glass carrier web. In the nitrogen-inerting study, oxygen levels were varied by placing samples on the carrier web and sending through the EB unit while purging the reaction chamber with N<sub>2</sub> gas. Samples were irradiated at 30-second intervals from 0 seconds (atmospheric conditions) to 150 seconds with a N<sub>2</sub> rate of 17 SCFM. Dose, web speed, and voltage were held constant at 30 kGy, 50 ft/min, and 200 kV, respectively. In the voltage study, polymer conversion as a function of depth was studied for various voltages (electron accelerations). Dose, belt speed, and O<sub>2</sub> level were held constant at 20 kGy, 50 ft/min, and <200 ppm, respectively.

#### *RT-Raman Spectroscopy*

RT-Raman Spectroscopy was used to identify a reference and a reaction peak to be used in conversion calculations. Samples were photopolymerized at ambient temperature in 1-mm ID quartz capillary tubes using an Acticure® Ultraviolet/Visible Spot Cure system (EXFO Photonic Solutions, Inc.). This system contains a high-pressure 100-W mercury vapor short arc lamp with a 250 – 400 nm wavelength filter; the effective irradiance was set at 50 mW/cm<sup>2</sup>. Real-time Raman spectra were gathered using a Mark II holographic probehead (Kaiser Optical Systems, Inc.) with a single-mode excitation fiber delivering ~220 mW of 785-nm near-infrared laser intensity to the sample through a 10x non-contact sampling objective. The probehead was connected to a HoloLab 5000R modular research

Raman spectrograph by a 100- $\mu\text{m}$  collection fiber. Spectra were collected continuously over 5 minutes with a 250-ms exposure time with 1 accumulation. Conversion,  $\alpha$ , was calculated using the formula

$$\alpha = 1 - \frac{I_{rxn}(t)/I_{ref}(t)}{I_{rxn}(0)/I_{ref}(0)} \quad (1)$$

where  $I_{rxn}(t)$  is the peak intensity of the reaction peak at time  $t$  and  $I_{ref}(t)$  is the peak intensity of the reference peak at time  $t$ .<sup>7</sup> This formula is valid for the real-time monitoring of reactions as well as conversion measurements taken post-cure. The inclusion of a reference peak eliminates instrument variation that occurs over time and the signal-to-noise (S/N) changes that can occur at increasing sample depths during depth profiling.

For the TMPTA/BADGEDA mixture, the reference peak was identified at  $1613\text{ cm}^{-1}$  (indicative of the  $-\text{C}=\text{C}-$  bond in the aromatic rings), and the reaction peak was identified at  $1636\text{ cm}^{-1}$  (indicative of the acrylate  $-\text{C}=\text{C}-$  bond). Real-time Raman spectroscopy confirmed these peak choices (see Figure 2): the peak intensity at  $1636\text{ cm}^{-1}$  decreases as the reaction progressed, while that at  $1613\text{ cm}^{-1}$  remained constant.

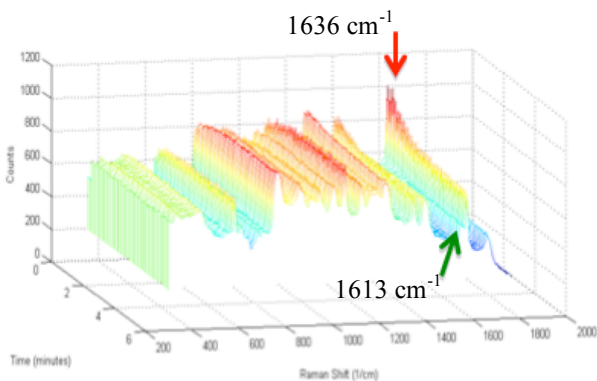


**Figure 2.** Real-time Raman spectra for photopolymerization of a 50/50 mixture of TMPTA and BADGEDA. A reaction peak of  $1636\text{ cm}^{-1}$  (red arrow) and a reference peak of  $1613\text{ cm}^{-1}$  (green arrow) were identified.

spectrograph (Kaiser Optical Systems, Inc.) via a 10- $\mu\text{m}$  confocal collection fiber. A single-mode excitation fiber was used to direct an incident beam of 785-nm near-infrared laser to the microscope. A beam intensity of  $\sim 8\text{ mW}$  was delivered to the sample through a 100x objective with a numerical aperture of 0.9 and a working distance of 0.27 mm. Monomer spectra were collected with an exposure time of 120 sec with 3 accumulations. The peak height of both the reaction and reference peak were averaged over 5 monomer spectra to provide accurate values for  $I_{rxn}(0)$  and  $I_{ref}(0)$ . Spectra for depth-profiling studies were also collected with a 120 sec

### Confocal Raman Microscopy

Confocal Raman microscopy was used to collect conversion as a function of depth for 70- $\mu\text{m}$  thick coatings. The confocal set-up consisted of a Leica DMLP optical microscope connected to a HoloLab 5000R modular research Raman

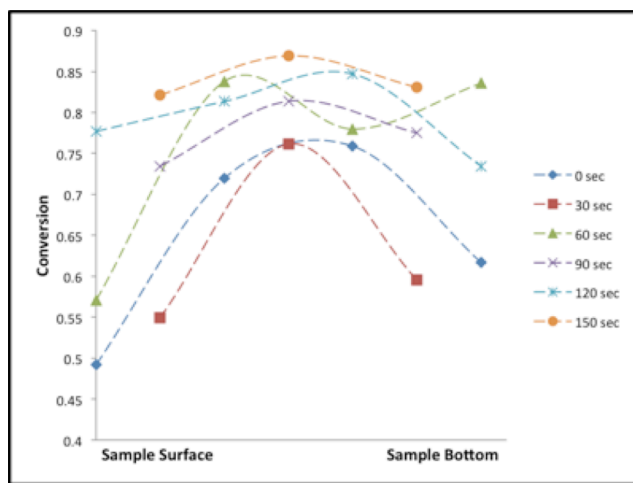


**Figure 3.** Depth profiles of samples with varying levels of  $\text{N}_2$  inertion (longer times = higher levels of  $\text{N}_2$ ). Surface conversion increases with increased  $\text{N}_2$  levels.

exposure time and 3 accumulations. A step size of 5  $\mu\text{m}$  was taken between spectra.

## Results and Discussion

### Nitrogen-inerting Study

Free-radical polymerization is known to be inhibited by molecular oxygen, which can scavenge initiator and polymer radicals, resulting in tacky films and coatings.<sup>8,9</sup> Both oxygen dissolved in the resin formulation and oxygen diffusing across the air/coating interface are problematic. However, diffused oxygen plays a greater role in EB-cured coatings since the concentration of free-radical active centers at the air/coating interface is much lower than in UV-cured films. In this nitrogen-inerting study, Raman confocal microscopy was used to show the effect of diffused oxygen on conversion throughout the film. As expected, at little to no  $\text{N}_2$ -inerting, surface conversions were suppressed to only 50-60% (Figure 3). As  $\text{N}_2$  levels were increased, surface conversion increased to a range of 75-85% conversion. However, the parabolic profile of the samples, which suggests a decrease in conversion at the sample bottom, was not expected. Decreased conversion at the sample bottom is not likely due to a decrease in energy deposition. The voltage used in this study, 200 kV, was specifically chosen because it provides enough electron acceleration to penetrate the full thickness of the sample (see 200 kV line in Figure 4). The decrease in conversion may be the result of monomer diffusion because, for these preliminary results, there was a delay of 3 months between curing and characterizing. These preliminary results will be confirmed with more immediate characterization.

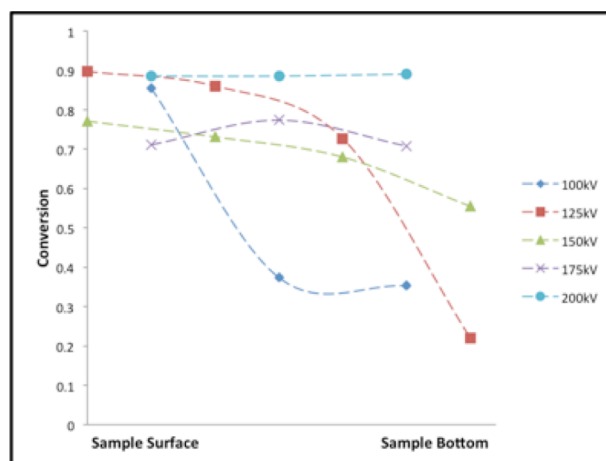


**Figure 4.** Depth profiles of samples processed at varying voltage levels. Conversion at the sample bottom increases with increasing voltage.

### Voltage Study

Because of its complexity, electron dose as a function of sample depth is often modeled using Monte Carlo simulations, which can be confirmed experimentally using dosimeters.<sup>10</sup> These simulations show that, unlike UV, the maximum energy deposition is beneath the sample surface. The depth of energy maximum is dependent on the voltage used; at higher voltages, the maximum is deeper in the sample. Low energy deposition at the surface is a result of the high energy of the electrons. Voltage also controls the depth of the energy deposition in a sample. Increasing the voltage increases the electron acceleration and the sample depth the electrons can penetrate. In this voltage study, Raman confocal microscopy was used to show how the electron acceleration affects the conversion depth profile. Samples were cured with good nitrogen inerting ( $<200$  ppm  $\text{O}_2$ ). At lower voltages, sample conversion at the sample bottom was significantly lower than the bulk due to inadequate electron acceleration (Figure 4). At higher voltages, a more consistent conversion is seen throughout the sample depth. These trends follow the energy deposition predicted by the theoretical Monte Carlo simulations. The energy deposited at a given location in the sample is roughly proportional to the concentration of free radicals at that location, which corresponds to the chain propagation and thus, monomer conversion.

## Conclusions

Characterization of EB polymerization is difficult because real-time monitoring techniques are not well suited for use in the EB environment. However, monitoring is needed in order to develop a fundamental understanding of EB-induced polymerization in order to make future processing and material advancements. The results of this study show that Raman depth profiling of monomer/oligomer conversion is promising for more thorough, quantitative analysis of these systems. The results of the oxygen inhibition study show a gradient in conversion predicted by oxygen diffusion into the samples. This characterization technique should be useful for future studies aimed at methods for reducing oxygen inhibition. The results of the voltage study show the gradient in polymer as a function of depth predicted by Monte Carlo simulation of energy deposition. This preliminary investigation sets the stage for future work in this area to develop a better understanding of the relationship among chemistry, processing parameters, and ultimate polymer properties for this system.

## Acknowledgments

This material is based upon work supported by the University of Iowa Math and Physical Sciences Funding Program.

## References

- (1) Datta SK, Chaki TK, Bhowmick AK, *Electron Beam Processing of Polymers*, 2000, pp. 1– 30.
- (2) Kinstle, J. F. In *Radiation Curing of Polymeric Materials*; Hoyle, C. E.; Kinstle, J. F., Eds.; ACS Symposium Series; American Chemical Society: Washington, DC, 1990; Vol. 417, pp. 17–23.
- (3) Drobny, J. G. *Ionizing Radiation and Polymers*; Elsevier Inc., 2013.
- (4) Dawes, K, Glover LC, “Effects of Electron Beam and Gamma Irradiation on Polymeric Materials,” *Physical Properties of Polymer Handbook*, edited by JE Mark, American Institute of Physics, pp. 557-576.
- (5) Richter KB, *Pulsed Electron Beam Curing of Polymer Coatings*, University of Minnesota, 2007.
- (6) Weiss D, Dunn D, Richter KB, Adler R, *Pulsed Electron Beam Polymerization*, 2005, pp. 1– 11.
- (7) Cai Y, Jessop, JLP, “Decreased Oxygen Inhibition in Photopolymerized Acrylate/Epoxy Hybrid Polymer Coatings as Demonstrated by Raman Spectroscopy,” *Polymer*, Vol. 47(19), 2006, pp. 6560-6566.
- (8) Odian G, *Principles of Polymerization*, 4<sup>th</sup> ed., John Wiley & Sons, Inc.: New York, 2004.
- (9) Fouassier, J. *Photoinitiation, Photopolymerization, and Photocuring: Fundamentals and Applications*; Hanser/Gardner Publication Inc.: Cincinnati, 1995.
- (10) Makuuchi, K.; Cheng, S. *Radiation Processing of Polymer Materials and its Industrial Applications*; John Wiley & Sons, Inc.: Hoboken, NJ, USA, 2012.